SPE
REPRINT
SERIES

No. 13
VOLUME I

GAS TECHNOLOGY

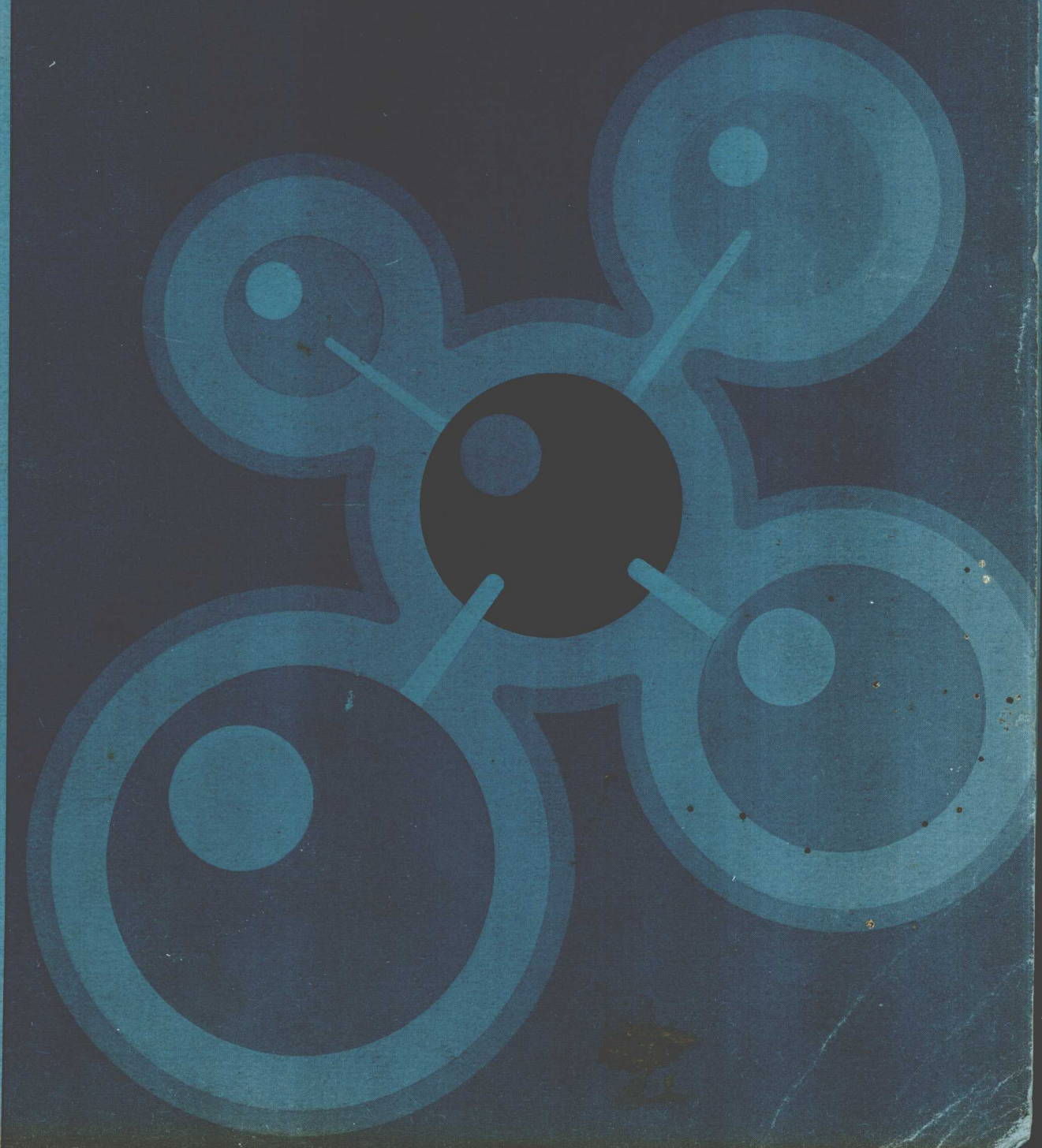

Published
by
the
Society
of
Petroleum
Engineers
of
AIME

SPE REPRINT SERIES NO. 13

Volume I

GAS TECHNOLOGY

1977 Edition

Published by the
Society of Petroleum Engineers of AIME
Dallas, Texas

PREFACE

Eighteen years have passed since the publication of the *Handbook of Natural Gas Engineering*, the premier work on the subject of gas technology. This has been a period not only of considerable increase in the value of gas but of substantial progress in the theory and practice of completing and producing gas wells and reservoirs.

The SPE Reprint Booklets on Gas Technology are intended to pick up where the *Handbook* left off, and bring to the reader the most up-to-date treatment of the subject.

The majority of the papers included in these volumes are application oriented. A few excellent papers are presented that treat the basic physics of gas flow and behavior.

The papers cover techniques suitable for both desk-calculator treatment and reservoir simulators. The simulation papers are presented, not with the idea of delving deeply into the formulation of models, but rather to show their practical application so that they might become a valuable tool to any engineer.

Space limits the number of papers that can be reprinted. The reader is directed to the bibliographies for the titles of many other fine papers, reprint booklets, and monographs on the subject of gas technology.

G. A. Mistrot

SPECIAL REPRINT COMMITTEE

TABLE OF CONTENTS

Part 1 — Reservoir Engineering

Part 2 — Gas Well Test Analysis

Part 3 — PVT

Part 1 — Reservoir Engineering

The selection of gas reservoir engineering papers for reprinting was made with the intent to present new and un-republished material that would be of immediate, practical use. The papers selected are essentially of two types: (1) techniques for use at the ''desk-calculator'' level, and (2) descriptions of how reservoir simulator programs for use on digital computers can be applied to gas reservoir studies. Three papers are ''case history'' studies.

One reprinted paper, ''Calculations of Unsteady-State Gas Flow Through Porous Media,'' published in 1953 by Bruce *et al.*, does not properly belong in either of the above categories. This outstanding paper is included because it contains useful fundamental information about the application of finite-difference techniques to gas reservoir flow problems. It should thus serve as an introduction to reservoir simulation for practicing reservoir engineers.

The paper ''Flow of Real Gases Through Porous Media,'' published in 1966 by Al-Hussainy *et al.*, introduced the concept of the real gas flow potential that greatly facilitated applying slightly compressible pressure transient theory to gas flow problems.

Frequently encountered problems discussed in other papers are (1) the calculation of bottom-hole pressures, (2) use of performance data to estimate gas in place, (3) significance and calculation of water influx in gas reservoirs, and (4) useful results that indicate how permeability is reduced by overburden pressure and water saturation in tight sandstones, thus relating core analysis permeability values to probable reservoir permeability values.

Papers dealing with the application of digital computer reservoir simulators show how such programs can be applied via trial-and-error history matching to the analysis and future performance prediction of wells and reservoirs. Two of the three ''case history'' papers deal with gas-cycling project studies.

Effect of Assumptions Used to Calculate Bottom-Hole Pressures in Gas Wells

KEITH L. YOUNG
JUNIOR MEMBER AIME

NORTHERN NATURAL GAS CO.
LIBERAL, KANS.

ABSTRACT

The general energy equation, including change in kinetic energy, was solved by numerical integration and used to evaluate simplifying assumptions and application practices over a wide range of conditions. When extreme conditions were encountered, sizable errors were caused by large integration intervals, application of Simpson's rule and neglecting change in kinetic energy. A maximum error of only 1.31 percent was caused by assuming temperature and compressibility constants at their average value. It was discovered that a discontinuity can develop in the integral for the injection case. This discontinuity indicates a point of zero pressure change and is an inflection point in the pressure traverse.

INTRODUCTION

When a pressure in a gas well is to be calculated, one of the first decisions is to select a method of calculation. In many instances, this selection becomes a problem because the literature, at best, provides an evaluation of any method for only a limited range of conditions. Once a method has been selected, a question often arises as to the size of the calculation interval which should be used. The question regarding calculation interval arises because an analytic solution is not obtainable and approximate solutions must be used.

This paper presents an evaluation of major assumptions and application practices of probably the two most widely used methods for calculating steady-state single-phase gas well pressures. The two methods are Cullender and Smith[1-6] (numerical integration), and average temperature and compressibility.[2-5,7] The Cullender-Smith method assumes that change in kinetic energy is negligible and is normally applied in two steps with a Simpson's rule correcton. The average temperature and compressibility method, in addition to neglecting kinetic energy change, asumes that temperature and compressibility are constant at their average values. This method is normally applied for wellhead shut-in pressures of less than 2,000 psi, and in one step.

Computer programs were written to compute bottom-hole pressure with and without the assumptions, using various approaches. Values of input parameters investigated are shown in Table 1. Flow rate was limited to a maximum of 5,000 and 10,000 Mcf/D for tubing sizes of 1.610 and 1.995 in. ID, respectively. Flow rate was also limited to 10,000 Mcf/D for a tubing size of 2.441 in. ID when wellhead flowing pressure was 100 psia. These limitations were imposed on flow rate so as not to exceed sonic velocity. The z factor routine available necessitated limiting bottom-hole temperature to 240F and wellhead pressure to 3,000 psia.

Pressures were compared on the basis of percent deviation from the trapezoidal integration of Eq. 1 or 2 at 100-ft intervals. A preliminary investigation indicated that a 1,000-ft interval solution would differ from a 50-ft interval solution by less than 0.25 percent; therefore, the 100-ft interval was chosen for a base. For the purpose of comparison, deviations less than 1 percent were considered insignificant.

EQUATIONS

Cullender and Smith give the equation for calculating pressure in a dry gas well, neglecting kinetic energy change, as

$$\frac{1{,}000\,\gamma L}{53.33} = \int_{p_{tf}}^{p_{wf}} \frac{p/Tz}{\dfrac{2.6665\,f q_{sc}^{\,2}}{d^5} + \dfrac{D}{L}\dfrac{(p/Tz)^2}{1{,}000}}\, d(p) \quad . \quad . \quad (1)$$

If change in kinetic energy is considered, Eq. 1 becomes

$$1{,}000\,L = \int_{p_{tf}}^{p_{wf}} \frac{\dfrac{53.33}{\gamma}\dfrac{p}{Tz} + \dfrac{111.1\,q_{sc}^{\,2}}{d^4 p}}{\dfrac{2.6665\,f q_{sc}^{\,2}}{d^5} + \dfrac{D}{L}\dfrac{(p/Tz)^2}{1{,}000}}\, d(p) \quad , \quad . \quad (2)$$

where $111.1\,q_{sc}^{\,2}/d^4 p$ = kinetic energy term. Eqs. 1 and 2 can be evaluated numerically at specific depths using the trapezoidal rule as shown by Cullender and Smith.

If change in kinetic energy is neglected and temperature and compressibility are assumed constant at their average values, Eq. 1 can be integrated to give the average temperature and compressibility equation,

$$p_{wf}^{\,2} = e^s\, p_{tf}^{\,2} + \frac{L}{D}\left[\frac{2.6665 f}{d^5} q_{sc}\, \bar{T}\, \bar{z}\right]^2 (e^s - 1) \quad , \quad . \quad (3)$$

where pressure squared is in thousands. Eq. 3 can be

Original manuscript received in Society of Petroleum Engineers office Sept. 8, 1966. Revised manuscript received Jan. 25, 1967. Paper (SPE 1626) was presented at SPE Gas Technology Symposium held in Omaha, Nebr., Sept. 15-16, 1966; and at SPE Amarillo Regional Meeting held in Amarillo, Tex., Oct. 27-28, 1966.

[1]References given at end of paper.

TABLE 1—VALUES OF PARAMETERS USED IN INVESTIGATION

Parameter	Values Used in Investigation					
Flow rate, Mcf/D	0	500	1,000	5,000	10,000	20,000
Wellhead pressure, psia	100	500	1,000	2,000	3,000	
Flow string ID, in.	1.610	1.995	2.441	4.000	4.950	
Specific gravity	0.550	0 650	0.750			
Wellhead temperature, °F	40	100				
Temperature gradient, °/ft	0.006	0.014				
Integration interval, ft	100	500	1,000	2,000	5,000	
Total depth, ft	10,000					

solved by making a one-step trial-and-error solution on $\bar{z}$.

Assumptions common to all three equations as used in this investigation are (1) steady-state turbulent flow, (2) gas as the single-phase flowing fluid, (3) straight-line temperature gradient and (4) friction factor constant over total length of pipe.

EFFECT OF SIZE OF INTEGRATION INTERVAL

Pressures were calculated using Eq. 2 for trapezoidal integration intervals of 100, 500, 1,000, 2,000 and 5,000 ft for a total of 228,336 pressures. The interval size of 100 ft accounted for 162,408 of these. Intervals larger than 100 ft accounted for the remaining 65,928 pressures.

Only 414 or 0.63 percent of the 65,928 pressures showed deviations greater than 1 percent. These deviations occurred at interval sizes of 2,000 and 5,000 ft and at wellhead pressures of 1,000 psia and less. The maximum deviation was 8.62 percent. In general, deviation is a maximum at high flow rate, low wellhead pressure, high specific gravity, low temperature and high temperature gradient. Fig. 1 is an example of how percent deviation increases with increasing integration interval size. Figs. 2 through 4 are examples of how percent deviation due to integration interval is influenced by flow rate, wellhead pressure and depth, respectively. Fig. 4 demonstrates that maximum deviation occurs at the first interval, regardless of the size.

EFFECT OF APPLYING SIMPSON'S RULE

In flowing gas wells, pressure is not always a linear function of depth. The nonlinear function occurs at low pressures and relatively high flow rates. This is caused by the second term in the denominator of Eq. 1 or 2 being insignificant at the surface but becoming significant with depth. When a nonlinear function exists, the size of the integration interval for Eqs. 1 and 2 should be reduced. Cullender and Smith suggested that application of Simpson's rule to a two-step calculation would give the approximate equivalent of a four-step calculation, even though pressure intervals may be unequal.

This investigation shows that application of Simpson's rule to a nonlinear pressure function tends to produce a pressure lower than a trapezoidal integration with small intervals. Fig. 5 shows an example of such a situation. The low reservoir pressure is caused by unequal pressure intervals. Pressure intervals in the upper portion of the wellbore will be larger than pressure intervals in the lower portion. In this situation, Simpson's rule improperly weights values of the integrand in Eq. 1 or 2. Cullender and Smith were apparently dealing with conditions where the error caused by Simpson's rule was approximately equal to the error caused by large intervals in the trapezoidal integration. These errors are opposite in sign.

EFFECT OF KINETIC ENERGY

If the kinetic energy term is neglected in Eq. 2, the integrand will be too small and the calculated pressure change too large. An example of neglecting kinetic energy change is given in Table 2. Using an integration interval of 100 ft, pressures with and without kinetic energy were calculated for all combinations of other parameters shown

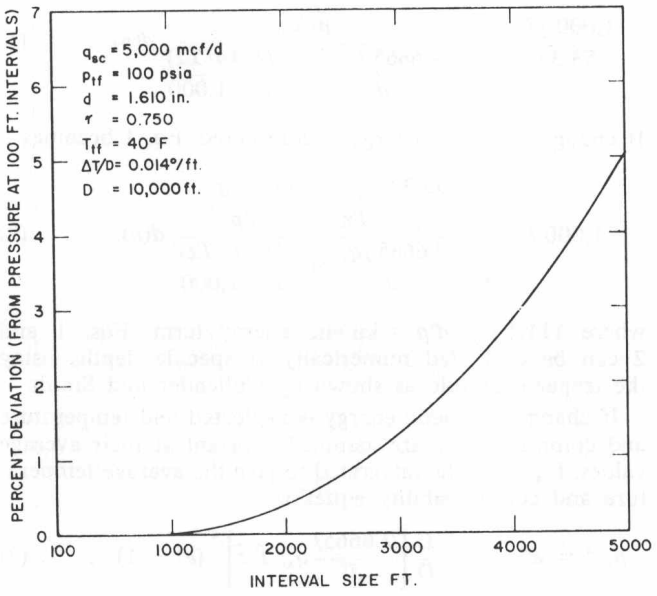

FIG. 1—EFFECT OF INTEGRATION INTERVAL.

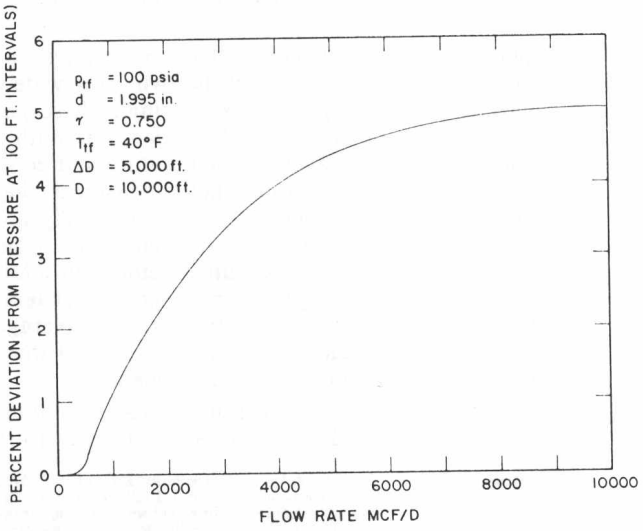

FIG. 2—EFFECT OF FLOW RATE ON DEVIATION DUE TO INTEGRATION INTERVAL.

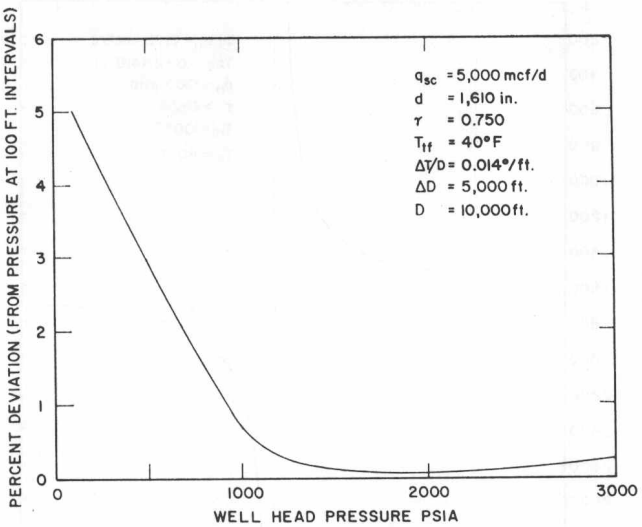

FIG. 3—EFFECT OF PRESSURE ON DEVIATION DUE TO INTEGRATION INTERVAL SIZE.

in Table 1 for 162,408 pressures. Of these pressures, 1,405 (0.87 percent) showed a deviation greater than 1 percent. Deviations greater than 1 percent did not occur below 4,000 ft, nor at wellhead pressures above 100 psia. The maximum deviation of 9.12 percent occurred at

Depth	100 ft
Flow rate	10,000 Mcf/D
Wellhead pressure	100 psia
Tubing diameter	1.995 in.
Specific gravity	0.750
Wellhead temperature	100F
Temperature gradient	0.014F/ft

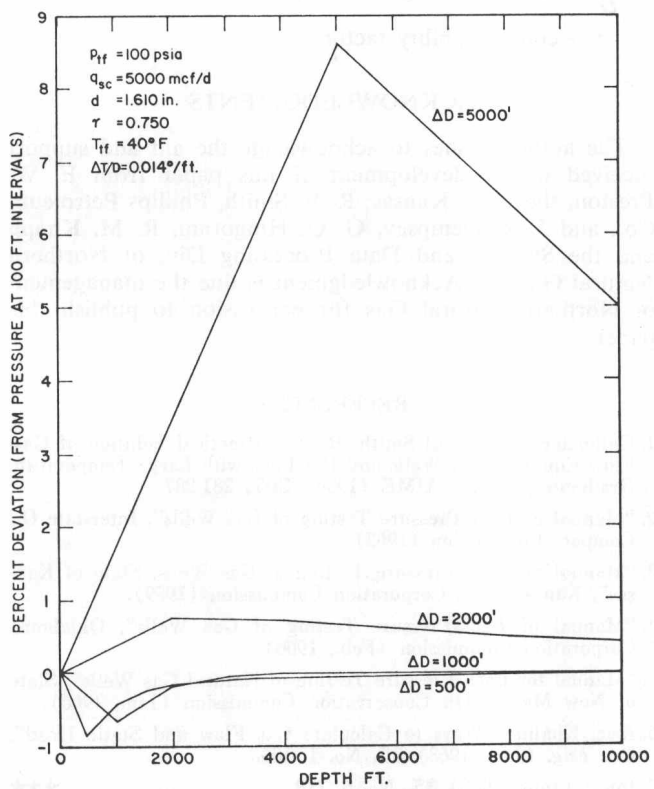

FIG. 4—EFFECT OF DEPTH ON DEVIATION DUE TO INTEGRATION INTERVAL SIZE.

TABLE 2—BOTTOM-HOLE PRESSURE COMPARISON WITH AND WITHOUT KINETIC ENERGY FROM 100-FT INTERVAL CALCULATIONS

q_{sc} = 10,000 Mcf/D Tbg ID = 1.995 in. T_{tf} = 100F

p_{tf} = 100 psia $\gamma = 0.750$ $\frac{\Delta T}{D} = 0.014°/ft$

Depth (ft)	Pressure With Kinetic Energy (psia)	Pressure Without Kinetic Energy (psia)	Percent Deviation
0	100.0	100.0	—
100	221.3	241.5	9.12
200	305.7	325.8	6.57
300	372.8	392.0	5.15
400	430.1	448.3	4.23
500	480.8	498.3	3.63
1,000	681.7	696.5	2.17
2,000	973.0	985.4	1.27
3,000	1,207.0	1,218.2	0.92
4,000	1,414.7	1,425.2	0.74
5,000	1,607.6	1,617.7	0.62
6,000	1,791.2	1,801.0	0.54
7,000	1,968.6	1,978.3	0.49
8,000	2,141.8	2,151.3	0.44
9,000	2,311.9	2,321.3	0.40
10,000	2,479.6	2,489.1	0.38

Bottom-hole flowing pressure:

With kinetic energy	221.3 psia
Without kinetic energy	241.5 psia.

The deviation in this example became less than 1 percent at a depth of 2,800 ft. This set of conditions is not likely to be encountered in actual practice.

Eq. 2 shows that the kinetic energy term is proportional to flow rate squared and inversely proportional to pressure and the fourth power of diameter.

EFFECT OF AVERAGE TEMPERATURE AND COMPRESSIBILITY

Eq. 3 was solved for depths of 4,000, 6,000, 8,000 and 10,000 ft. Values of other parameters used are shown in

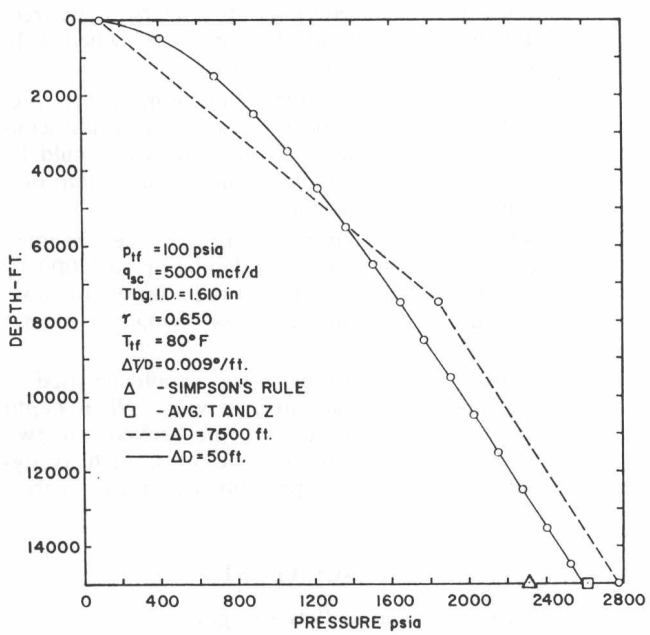

FIG. 5—COMPARISON OF SOLUTIONS FOR BOTTOM-HOLE PRESSURE.

Table 1. A total of 6,432 pressures were calculated from Eq. 3. When compared with pressures from the trapezoidal integration at 100-ft intervals and neglecting kinetic energy, 42 (0.65 percent) of the pressures deviated by more than 1 percent. All of these deviations except one occurred for conditions of

Wellhead pressure	2,000 and 3,000 psia
Wellhead temperature	40F
Temperature gradient	0.014 F/ft
Specific gravity	0.750
Depth	10,000 ft.

The maximum deviation of 1.31 percent occurred at a wellhead pressure of 2,000 psia and a flow rate of zero. Deviations for a wellhead pressure of 3,000 psia were less than those for 2,000 psia. This indicates that deviations will probably not increase for pressures above 3,000 psi. It should be noted that the maximum deviation caused by assuming average temperature and compressibility is considerably less than that caused by neglecting kinetic energy, large integration intervals or application of Simpson's rule (Fig. 5).

INJECTION CASE

For injection, D/L in Eqs. 1 and 2 is negative. In this case, the denominator of the integrand can become zero and the integrand goes to infinity. Fig. 6 is a plot of integrand I as a function of depth and shows the discontinuity which can develop. When a discontinuity occurs, change in pressure over that one interval may be assumed equal to zero and becomes an inflection point in the pressure traverse.

CONCLUSIONS

1. An integration interval of 1,000 ft should be used to assure accurate trapezoidal integration of Eq. 2 or 3.

2. Simpson's rule should not be applied in an effort to correct for large trapezoidal integration intervals.

3. If flowing pressure at total depth is the desired quantity, change in kinetic energy may be ignored when depth is greater than 4,000 ft or wellhead flowing pressure is above 100 psia. If an accurate pressure traverse is desired, change in kinetic energy should be considered when wellhead flowing pressure is below 500 psia.

4. A discontinuity can develop when numerically integrating Eq. 2 or 3 for the injection case. When a discontinuity occurs, pressure change in that interval should be set equal to zero. Also, it should be noted that Simpson's rule cannot be applied in this situation.

5. Temperature and compressibility can be assumed constant at their average values for depths up to 8,000 ft. The average temperature and compressibility method, however, should not be applied unless change in kinetic energy is insignificant.

For all normal field situations, Eq. 3 should be used to calculate bottom-hole pressure in gas wells. When depth exceeds 8,000 ft, the calculation may be broken into two or more intervals. When unusual conditions, such as significant kinetic energy change, prohibit use of Eq. 3, then Eq. 2 should be used.

NOMENCLATURE

d = internal diameter of flow string, in.

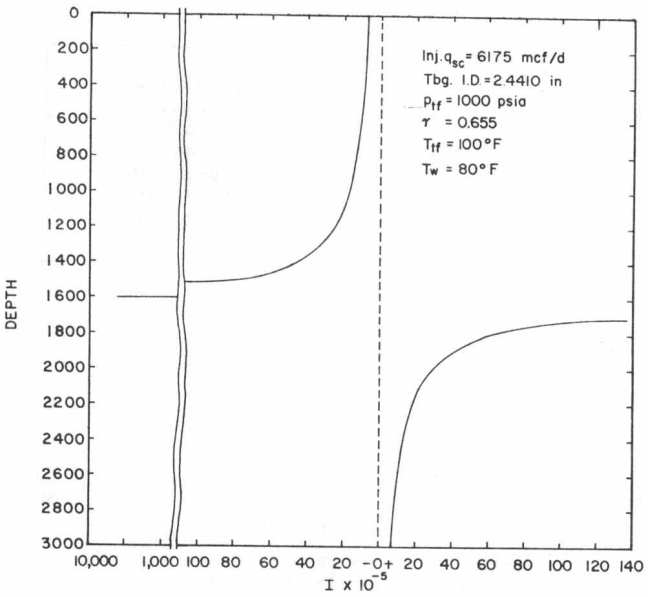

FIG. 6—DISCONTINUITY FOR INJECTION CASE.

e = 2.7183

D = vertical depth, ft

ΔD = trapezoidal integration interval, ft

I = integrand of Eq. 2

L = length of flow string, ft

p = pressure, psia

q_{sc} = flow rate, MMcf/D at 14.65 psia and 60F

$S = 0.0375 \frac{\gamma D}{\bar{T}\bar{z}}$

T = temperature, °R

$\frac{\Delta T}{D}$ = temperature gradient, °/ft

z = compressibility factor

ACKNOWLEDGMENTS

The author wishes to acknowledge the aid and support received in the development of this paper from F. W. Preston, the U. of Kansas; R. V. Smith, Phillips Petroleum Co.; and J. R. Dempsey, G. G. Hingorani, R. M. Knapp and the Systems and Data Processing Div. of Northern Natural Gas Co. Acknowledgment is due the management of Northern Natural Gas for permission to publish this paper.

REFERENCES

1. Cullender, M. H. and Smith, R. V.: "Practical Solution of Gas-Flow Equations for Wells and Pipelines with Large Temperature Gradients", *Trans.*, AIME (1956) **207,** 281-287.

2. "Manual of Back-Pressure Testing of Gas Wells", Interstate Oil Compact Commission (1962).

3. "Manual of Back Pressure Testing of Gas Wells, State of Kansas", Kansas State Corporation Commission (1959).

4. "Manual of Back-Pressure Testing of Gas Wells", Oklahoma Corporation Commission (Feb., 1966).

5. "Manual for Back-Pressure Testing of Natural Gas Wells", State of New Mexico Oil Conservation Commission (Jan., 1966).

6. Aziz, Khalid: "Ways to Calculate Gas Flow and Static Head", *Pet. Eng.* (Jan., 1963) **35,** No. 1, 106.

7. Ibid.: (June, 1963) **35,** No. 6, 118.

★★★

CALCULATIONS OF UNSTEADY-STATE GAS FLOW THROUGH POROUS MEDIA

G. H. BRUCE, D. W. PEACEMAN AND H. H. RACHFORD, JR., JUNIOR MEMBER AIME, HUMBLE OIL AND REFINING CO., HOUSTON, TEX.; AND J. D. RICE, THE RICE INSTITUTE, HOUSTON, TEX.

ABSTRACT

The problem of unsteady-state gas flow through porous media leads to a second-order non-linear partial differential equation for which no analytical solution has been found. In this paper a stable numerical procedure is developed for solving the equation for production of gas at constant rate from linear and radial systems. An electronic digital computer is used to perform the numerical integration using an implicit form of an approximating difference equation. Solutions are presented in graphical form for various values of dimensionless parameters. The solutions are compared with the laboratory study of gas depletion in a linear system.

INTRODUCTION

Production of fluids from porous rock reservoirs is essentially a transient process. Transient gradients develop as soon as production begins, and further withdrawals continue to cause disturbances which propagate throughout the reservoir, each adding in some way to the prior ones.

A correct mathematical analysis of this behavior is complicated by the fact that the transient or unsteady-state flow of compressible fluids must be described by difficult second-order partial differential equations. As a practical matter, three distinctly different cases arise:

1. Flow of single-phase liquid
2. Flow of gases
3. Multiphase flow

The first of these has been found to give a linear second-order equation similar to the well-known heat flow equation.

$$\nabla^2\gamma = \alpha \frac{\partial \gamma}{\partial \theta} \quad \ldots\ldots\ldots\ldots \quad (1)$$

where γ is fluid density, θ is time, and α a constant for the system, provided $d\gamma = \gamma\, c\, dp$, where the compressibility, c, is constant over the range of pressure, p, considered. Solutions of Equation (1) for both linear and radial flow are available in several forms.[2,3,4]

On the other hand, the second case, which is the flow of gas, gives a non-linear second-order equation,

$$\nabla^2 p^2 = \alpha \frac{\partial p}{\partial \theta} \quad \ldots\ldots\ldots\ldots \quad (2)$$

the solution of which is not known. Although a number of approximate solutions have been proposed,[1,3,6] each is limited in value by the associated simplifying assumptions.

Inasmuch as the analysis of transient flow is limited to liquid systems, a solution of the second case is necessary if further progress is to be made in studying underground fluid movement. For this reason a solution of Equation (2) was undertaken by means of numerical integration of approximating difference equations.

BASIC DIFFERENTIAL EQUATION

Equation (2) is derived by combining the equation of continuity,

$$\nabla(\gamma \vec{v}) = -\phi \frac{\partial \gamma}{\partial \theta} \quad \ldots\ldots\ldots\ldots \quad (3)$$

the perfect gas law,

$$\gamma = \frac{p}{RT} \quad \ldots\ldots\ldots\ldots \quad (4)$$

and Darcy's law

$$\vec{v} = -\frac{K}{\mu} \nabla p \quad \ldots\ldots\ldots\ldots \quad (5)$$

to give the basic differential equation

$$\nabla^2 p^2 = \frac{2\phi\mu}{K} \frac{\partial p}{\partial \theta} \quad \ldots\ldots\ldots\ldots \quad (2')$$

Strictly speaking, the fluids present in a gas reservoir are not perfect gases. Furthermore, there are indications that over certain velocity ranges, Darcy's law is not applicable. It would not be practicable, however, to attempt to obtain numerical solutions which would take into account all the possible variations from these laws which could occur in actual systems. The

[1]References given at end of paper.

Manuscript received in the Petroleum Branch office Aug. 12, 1952. Paper presented at the Petroleum Branch Fall Meeting in Houston, Tex., Oct. 1-3, 1952.

methods which are developed here for the solution of Equation (2) in the ideal case can be extended to the solution of specific problems where the gases exhibit more complicated behavior. Two cases are considered in this paper, linear flow and radial flow, both with constant production rate.

LINEAR FLOW

For linear flow, Equation (2′) reduces to

$$\frac{\partial^2 p^2}{\partial x^2} = \frac{2\phi\mu}{K}\frac{\partial p}{\partial \theta} \quad . \quad . \quad . \quad . \quad . \quad . \quad . \quad . \quad (6)$$

with initial condition

$$\theta = 0 \qquad p = p_i \quad . \quad . \quad . \quad . \quad . \quad . \quad . \quad . \quad . \quad (7)$$

and the boundary conditions

$$x = 0, \quad q = \frac{Ka}{\mu RT} p \frac{\partial p}{\partial x} \quad . \quad . \quad . \quad . \quad . \quad . \quad . \quad (8)$$

$$x = L, \quad p\frac{\partial p}{\partial x} = 0 \quad . \quad . \quad . \quad . \quad . \quad . \quad . \quad . \quad (9)$$

where q is the molar rate of production, a is the cross-sectional area, and L is the length of the reservoir. Equation (8) follows from the application of Equations (4) and (5) to the producing boundary, while Equation (9) follows from the absence of flow across the closed boundary.

Dimensionless Differential Equation

By making the substitutions

$$P = \frac{p}{p_i} \quad . \quad . \quad . \quad . \quad . \quad . \quad . \quad . \quad . \quad . \quad . \quad (10)$$

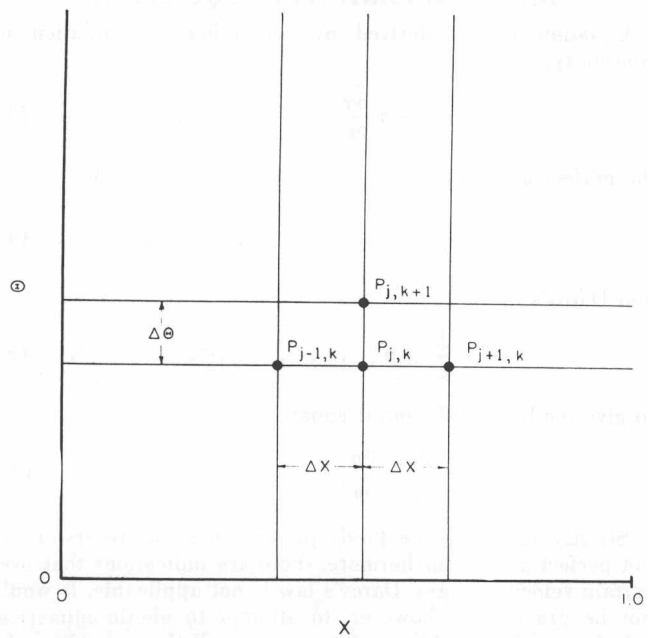

FIG. 1 — INTEGRATION NET FOR LINEAR RESERVOIR.

$$X = \frac{x}{L} \quad . \quad . \quad . \quad . \quad . \quad . \quad . \quad . \quad . \quad . \quad . \quad (11)$$

$$\Theta = \frac{p_i K\theta}{2L^2\phi\mu} \quad . \quad . \quad . \quad . \quad . \quad . \quad . \quad . \quad . \quad . \quad (12)$$

$$Q = \frac{-\dfrac{dN}{d\Theta}}{N_i} = \frac{2qL\mu RT}{p_i^2 Ka} \quad . \quad . \quad . \quad . \quad . \quad . \quad . \quad (13)$$

where N is the number of mols remaining in the reservoir at any time, Equations (6) through (9) are reduced to dimensionless form

$$\frac{\partial^2 P^2}{\partial X^2} = \frac{\partial P}{\partial \Theta} \quad . \quad . \quad . \quad . \quad . \quad . \quad . \quad . \quad . \quad . \quad (14)$$

with initial condition

$$\Theta = 0, \quad P = 1 \quad . \quad . \quad . \quad . \quad . \quad . \quad . \quad . \quad . \quad . \quad (15)$$

and boundary conditions

$$X = 0, \quad \frac{\partial P^2}{\partial X} = Q \quad . \quad . \quad . \quad . \quad . \quad . \quad . \quad . \quad (16)$$

$$X = 1, \quad \frac{\partial P^2}{\partial X} = 0 \quad . \quad . \quad . \quad . \quad . \quad . \quad . \quad . \quad (17)$$

The dimensionless rate parameter, Q, is sufficient to characterize the problem. Its significance may be understood more clearly by considering that $Q\Theta$ represents the fraction of the original gas which has been removed at any dimensionless time, Θ.

Difference Equation

Approximate solutions of differential equations may be obtained by evaluating the derivatives in terms of finite differences and integrating numerically by means of the resulting difference equations. To formulate a difference equation for Equation (14), a net of mesh-width $\triangle X$ and $\triangle\Theta$ is established as shown in Fig. 1. Subscripts j and k are used to denote distance and time positions, respectively, as $P_{j,k}$. Approximations to X-derivatives at j,k are found by the Taylor expansions of P^2 about point j,k:

$$P^2_{j+1,k} = P^2_{j,k} + \frac{\partial P^2}{\partial X}\triangle X + \frac{\partial^2 P^2}{\partial X^2}\frac{\overline{\triangle X}^2}{2!} + \ldots \quad . \quad (18)$$

$$P^2_{j-1,k} = P^2_{j,k} - \frac{\partial P^2}{\partial X}\triangle X + \frac{\partial^2 P^2}{\partial X^2}\frac{\overline{\triangle X}^2}{2!} - \ldots \quad . \quad (19)$$

Addition of Equations (18) and (19), neglecting terms of the order of $\dfrac{\partial^4 P^2}{\partial X^4}\dfrac{\overline{\triangle X}^4}{4!}$ and higher, gives

$$\frac{\partial^2 P^2}{\partial X^2} = \frac{\triangle^2_{j,k}(P^2)}{\overline{\triangle X}^2} \quad . \quad . \quad . \quad . \quad . \quad . \quad . \quad . \quad (20)$$

where $\triangle^2_{j,k}(P^2)$ implies $P^2_{j+1,k} + P^2_{j-1,k} - 2P^2_{j,k}$

Expanding $P_{j,k+1}$ about $P_{j,k}$ and neglecting the second- and higher-order terms gives

$$\frac{\partial P}{\partial \Theta} = \frac{P_{j,k+1} - P_{j,k}}{\triangle\Theta} \quad . \quad . \quad . \quad . \quad . \quad . \quad . \quad . \quad (21)$$

Predictive Form

Equating Equations (20) and (21) in accordance with Equation (14) and solving for $P_{j,k+1}$ yields the predictive relation

$$P_{j,k+1} = \frac{1}{\rho}\Delta_{j,k}^2(P^2) + P_{j,k} \quad . \quad . \quad . \quad . \quad (22)$$

where $\rho = \dfrac{\overline{\Delta X}^2}{\Delta\Theta}$.

Equation (22) is explicit for $P_{j,k+1}$ in terms of the pressures at time step k. For a known P(X,0) the set $P_{1,1} \ldots P_{n,1}$ may be computed by Equation (22). The boundary $P_{0,1}$ and $P_{n+1,1}$ may be computed from a difference form of the boundary conditions

$$\frac{P_1^2 - P_0^2}{\Delta X} = Q \quad . \quad . \quad . \quad . \quad . \quad . \quad . \quad . \quad . \quad (23)$$

$$\frac{P_{n+1}^2 - P_n^2}{\Delta X} = 0 \quad . \quad . \quad . \quad . \quad . \quad . \quad . \quad . \quad . \quad (24)$$

Equations (22), (23) and (24) with $k = 0$ produce a $P(X, \Theta_1)$. Repetition of this purely predictive calculation for succeeding time steps yields the solution, $P(X, \Theta)$. Unfortunately, use of these simple equations is severely restricted for practical calculations as will be shown in the following section.

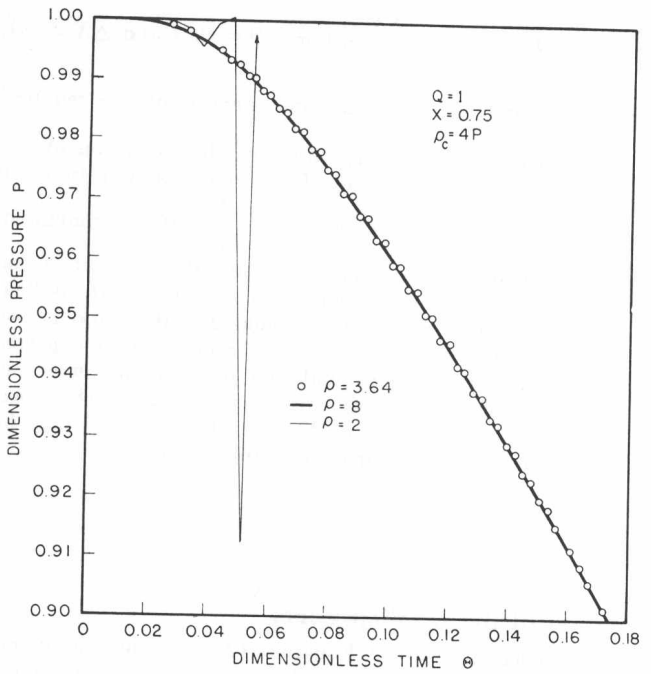

FIG. 2 — COMPARISON OF P (0.75,Θ) FOR THE LINEAR RESERVOIR CALCULATED USING THE PREDICTIVE EQUATION (22) WITH THREE VALUES OF MESH-RATIO.

Errors

Two independent errors arise in the foregoing solution: truncation of the series of Equations (18) and (19) by omission of the high-order terms, and growth of the elemental rounding errors in repeated applications of Equations (22), (23) and (24). Truncation errors can be estimated by studying the size of the neglected high-order terms. Errors from this source may be limited by choice of small mesh-widths or inclusion of higher-order differences in Equations (22), (23) and (24).

Growth of elemental rounding errors is a more serious matter, for this may occur in any calculation where results of one calculation are subjected repeatedly to subsequent applications of difference equations. An analysis similar to that used by O'Brien, Hyman and Kaplan[5] for studying error growth is presented in the Appendix and shows the limitations in using Equation (22). This analysis leads to the conclusion that a sufficient condition to prevent error growth is

$$\rho \geqslant 4P_k \quad . \quad . \quad . \quad . \quad . \quad . \quad . \quad . \quad . \quad . \quad . \quad . \quad . \quad (25)$$

This implies that in addition to choosing a mesh size small enough to limit truncation error, the mesh ratio, $\dfrac{\Delta X}{\Delta\Theta}$, must also be chosen properly. Violation of the inequality of Equation (25) leads to the unstable situation in which the growth of small rounding errors swamps the calculations. This condition is referred to as "computational instability."

It is interesting to compare the solution $P(X, \Theta)$ computed for $Q = 1$ by Equation (22) for several values of ρ. Fig. 2 is a plot of $P(0.75, \Theta)$ for three values of ρ. The critical ratio ρ_c is $4P$. For $\rho = 2$, the solution shows violent instability. For $\rho = 8$, a stable solution is obtained. For $\rho = 3.64$, a mild oscillation develops, but as P diminishes ρ_c falls below 3.64, the errors decay, and the solution converges back toward the stable solution.

The existence of ρ_c is inconvenient for practical computing, for if a small ΔX is chosen to give low truncation error, a small $\Delta\Theta$ is required for stability. For example, with a ΔX of 0.1, the permissible $\Delta\Theta$ is 0.0025. If $Q = 0.01$, 20,000 time steps would be required to remove half the gas.

Implicit Form

If Equation (20) is rewritten

$$\frac{\partial^2 P^2}{\partial X^2} = \frac{\Delta_{j,k}^2(P^2) + \Delta_{j,k+1}^2(P^2)}{2\overline{\Delta X}^4} \quad . \quad . \quad . \quad . \quad . \quad (26)$$

the second derivative of Equation (26) is centered at a time step $k+\frac{1}{2}$, and Equation (21) becomes second-order correct. Combining Equation (26) with Equation (21) gives

$$P_{j,k+1} - \frac{1}{2\rho}\Delta_{j,k+1}^2(P^2) = P_{j,k} + \frac{1}{2\rho}\Delta_{j,k}^2(P^2) \quad . \quad . \quad (27)$$

which is now implicit in the unknowns at step $k+1$. Von Neumann has shown the stability of implicit formulas. The analysis of error growth, which is presented in the Appendix, shows that a sufficient condition for the prevention of error growth in Equation (27) is

$$P_k - P_{k+1} \leqslant \frac{\rho}{2} \quad . \quad . \quad . \quad . \quad . \quad . \quad . \quad . \quad . \quad . \quad (28)$$

where P_k is the average pressure at Θ_k. That is, the average pressure may decline no more than $\dfrac{\rho}{2}$ for the associated time step $\Delta\Theta$. Since $Q\Delta\Theta \cong P_k - P_{k+1}$, the condition of Equation

(28) is met if $\Delta\Theta = \frac{\Delta X}{\sqrt{2Q}}$. For a $Q = 0.01$ and $\Delta X = 0.1$, $\Delta\Theta = \frac{1}{\sqrt{2}}$, and only 71 equal time steps would be required to remove half the gas while satisfying this condition of stability. Further, the magnitude of the error amplification can be at worst no larger than the ratio $\frac{P_k}{P_{k+1}}$; if this maximum amplification operates at every time step, the cumulative amplification may not exceed the ratio of the initial to final pressure. In removing half the original gas, this ratio is two and error growth from amplification is about 1/70 the expected growth from statistical accumulation of rounding errors in 20,000 steps using the predictive equation, (22). Therefore, in integrating with Equation (27) the choice of $\Delta\Theta$ may be made with minor regard for error amplification.

Solution of the Implicit Form

In applying the implicit Equation (27), an integration net is set up so that the producing boundary ($X = 0$) is at the midpoint of the interval between X_0 and X_1 while the closed boundary ($X = 1$) is at the midpoint of the interval between X_n and X_{n+1}. The two boundary equations, (23) and (24), together with the implicit equation, (27), written for each of the points, $X_0, X_1 \ldots X_n$, form a set of $n+2$ simultaneous, non-linear equations which must be solved for $P_{0,k+1}, P_{1,k+1}, \ldots P_{n+1,k+1}$. In the remainder of this section, it will be understood that time step $k+1$ is under discussion, and the subscript $k+1$ will be omitted. Elimination of P_{n+1} and rearrangement give the following $n+1$ equations:

$$\left.\begin{aligned} &P_0^2 - P_1^2 = -Q\Delta X \\ &-P_{j-1}^2 + 2P_j^2 + 2\rho P_j - P_{j+1}^2 = D_j \quad 1 \leqslant j \leqslant n-1 \\ &-P_{n-1}^2 + P_n^2 + 2\rho P_n = D_n \end{aligned}\right\} \quad (29)$$

where D_j and D_n are defined by

$$D_j = 2\rho P_{j,k} + P_{j-1,k}^2 - 2P_{j,k}^2 + P_{j+1,k}^2 \quad \ldots \quad (30)$$

$$D_n = 2\rho P_{n,k} + P_{n-1,k}^2 - P_{n,k}^2 \quad \ldots \quad (31)$$

The method used here for solving these equations consists of factoring the non-linear terms into a product of assumed values of P and unknown values of P. The resulting linear simultaneous equations may be solved for the unknown P's. These values may then be used as assumed values of P for the next iteration. The iterations are continued until the unknown values are equal to the assumed values.

Let P_j^* be the assumed value of P_j. The non-linear terms in Equation (29) are all present as differences of squares, which may be factored in three different ways. For example

$$P_j^2 - P_{j-1}^2 = P_j^* P_j - P_{j-1}^* P_{j-1} \quad \ldots \quad (32a)$$

$$P_j^2 - P_{j-1}^2 = (P_j^* + P_{j-1}^*)(P_j - P_{j-1}) \quad \ldots \quad (32b)$$

$$P_j^2 - P_{j-1}^2 = (P_j^* - P_{j-1}^*)(P_j + P_{j-1}) \quad \ldots \quad (32c)$$

The choice of the method of factoring depends upon the rapidity with which the iterations of the resulting equations converge. As shown in the Appendix, the first method may converge or diverge slowly, the second method, in general, converges rapidly, while the third method diverges rapidly. Accordingly, the second method, (32b), of factoring is used with all the equations of (29). The following set of linear simultaneous equations results:

$$\left.\begin{aligned} &P_0(P_0^* + P_1^*) - P_1(P_0^* + P_1^*) = -Q\Delta X \\ &-P_{j-1}(P_{j-1}^* + P_j^*) + P_j(P_{j-1}^* + 2P_j^* + P_{j+1}^* + 2\rho) - \\ &\quad P_{j+1}(P_j^* + P_{j+1}^*) = D_j \quad 1 \leqslant j \leqslant n-1 \\ &-P_{n-1}(P_{n-1}^* + P_n^*) + P_n(P_{n-1}^* + P_n^* + 2\rho) = D_n \end{aligned}\right\} \quad (33)$$

The problem remains of solving the simultaneous equations, (33). L. H. Thomas of the Watson Scientific Computing Laboratory has suggested a method for solving this type of system of linear equations. While the method is equivalent to plain Gaussian elimination, it avoids the error growth associated with the back solution of the elimination method and also minimizes the storage problems in machine computation. The method may be summarized as follows. For a system of equations,

$$\left.\begin{aligned} &B_0 P_0 + C_0 P_1 = D_0 \\ &A_j P_{j-1} + B_j P_j + C_j P_{j+1} = D_j \quad 1 \leqslant j \leqslant n-1 \\ &A_n P_{n-1} + B_n P_n = D_n \end{aligned}\right\} \quad (34)$$

let

$$\left.\begin{aligned} &w_0 = B_0 \\ &w_j = B_j - A_j b_{j-1} \qquad 1 \leqslant j \leqslant n \end{aligned}\right\} \quad (35)$$

$$b_j = \frac{C_j}{w_j} \qquad 0 \leqslant j \leqslant n-1 \quad \ldots \quad (36)$$

and

$$\left.\begin{aligned} &g_0 = \frac{D_0}{w_0} \\ &g_j = (D_j - A_j g_{j-1})/w_j \qquad 1 \leqslant j \leqslant n \end{aligned}\right\} \quad (37)$$

The solution is

$$\left.\begin{aligned} &P_n = g_n \\ &P_j = g_j - b_j P_{j+1} \qquad 0 \leqslant j \leqslant n-1 \end{aligned}\right\} \quad (38)$$

Thus w, b and g are computed in order of increasing j, and P is then computed in order of decreasing j. The proof of the method is shown in the Appendix.

Comparing Equations (34) with Equations (33), and applying Equations (35), (36) and (37), yields

$$\left.\begin{aligned} &b_0 = -1 \\ &b_j = -\frac{P_j^* + P_{j+1}^*}{P_{j-1}^* + 2P_j^* + P_{j+1}^* + 2\rho + (P_{j-1}^* + P_j^*)b_{j-1}} \quad 1 \leqslant j \leqslant n-1 \end{aligned}\right\} \quad \ldots \quad (39)$$

$$\left.\begin{aligned} &g_0 = -\frac{Q\Delta X}{P_0^* + P_1^*} \\ &g_j = \frac{D_j + (P_{j-1}^* + P_j^*)g_{j-1}}{P_{j-1}^* + 2P_j^* + P_{j+1}^* + 2\rho + (P_{j-1}^* + P_j^*)b_{j-1}} \quad 1 \leqslant j \leqslant n-1 \\ &g_n = \frac{D_n + (P_{n-1}^* + P_n^*)g_{n-1}}{P_{n-1}^* + P_n^* + 2\rho + (P_{n-1}^* + P_n^*)b_{n-1}} \end{aligned}\right\} \quad \ldots \quad (40)$$

From Equation (39), it can be seen that the values of $-b_j$ are equal to or less than one. Consequently, the computation of the successive values of b_j and g_j will be free from error growth. By referring to Equation (38), it can be seen that the computation of the successive values of P_j will also be free from error growth.

The numerical procedure, then, consists in starting with $P_j = 1$ for all j at $\Theta = 0$, calculating $P_{j,1}$, using these values to calculate $P_{j,2}$, and so on. The procedure for using P_j at $\Theta = \Theta_k$ to calculate the P_j at $\Theta = \Theta_{k+1}$ is as follows: The constants ρ, $Q\triangle X$, D_1, . . . D_n are evaluated from their definitions. The predictive equation, (22), is used to calculate trial values of $P_{j,k+1}$ which are used as the first assumed values for P_j^* in Equations (39) and (40) to calculate b's and g's; these, in turn, are used in Equation (38) to calculate new values of $P_{j,k+1}$. These are then substituted for P_j^* in Equations (39) and (40) and the calculation of b's, g's, and finally of P's is repeated. This process is repeated until there is no significant change in the P's. Generally, five iterations are sufficient.

Results

Using the procedures developed in the preceding section, the numerical integration of Equation (14) was carried out using an IBM Card-Programmed Calculator which was wired to perform eight-digit, floating-decimal arithmetic. Pressure distributions for linear unsteady-state gas flow were calculated for seven values of Q: 2, 1, 0.5, 0.2, 0.1, 0.05, and 0.02. For the case of $Q = 1$, results obtained with the implicit difference equations, using Equations (38), (39) and (40), were found to compare well with results obtained with the predictive equation, (22). In both cases, 10 distance increments were used. In addition, to examine the truncation error in the distance direction, results obtained with the predictive equation for 10 distance increments were compared with those obtained with the predictive equation for 20 distance increments, and again good agreement was obtained. For the case of $Q = 2$, the predictive equation with 20 distance increments was used. For all the remaining values of Q, the implicit difference equations with 10 distance increments were used. In carrying out the solutions, small time steps were used at the beginning, where the time derivatives were highest, and continually increased as the solution progressed. For example, for the case of $Q = 0.5$, 35 time steps were used; $\triangle\Theta$ had the value 0.0001 for five steps, 0.0005 for three steps, 0.002 for four steps, 0.01 for nine steps, 0.05 for eight steps, and 0.1 for the last six steps. Results for the seven values of Q are presented in Figs. 3a through 3g. As an independent check on the calculations, a total material balance was made after each time step by evaluating numerically the integral $\int_0^1 (1-P)\,dX$ and comparing with $Q\Theta$. Agreement was within 0.15 per cent of the gas remaining.

In Fig. 4, comparison is made between calculated solutions and experimental data obtained in the laboratory. The laboratory test equipment consisted of a linear system of one-in. standard galvanized steel pipe packed with sand. Pressure gauges were located at the outflow and closed ends and at four positions along the pipe. The overall length of the system

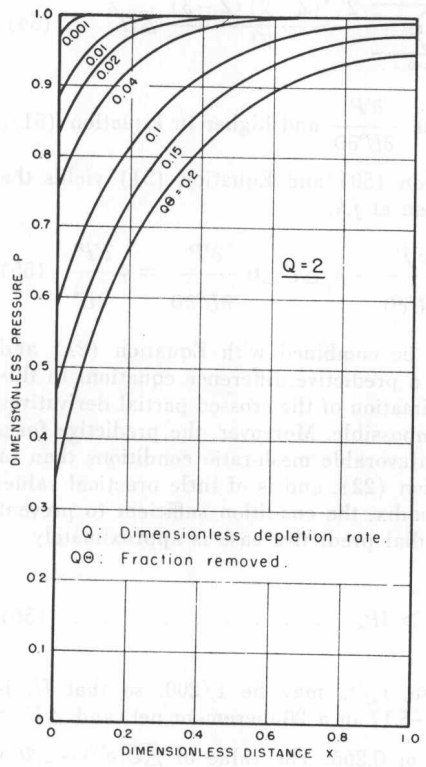

FIG. 3a — CALCULATED PRESSURE DISTRIBUTION FOR DEPLETION OF LINEAR GAS RESERVOIR. Q = 2.

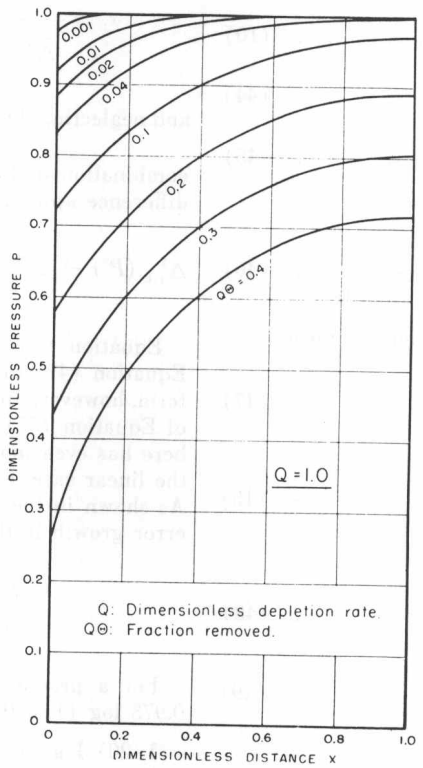

FIG. 3b — CALCULATED PRESSURE DISTRIBUTION FOR DEPLETION OF LINEAR GAS RESERVOIR. Q = 1.0.

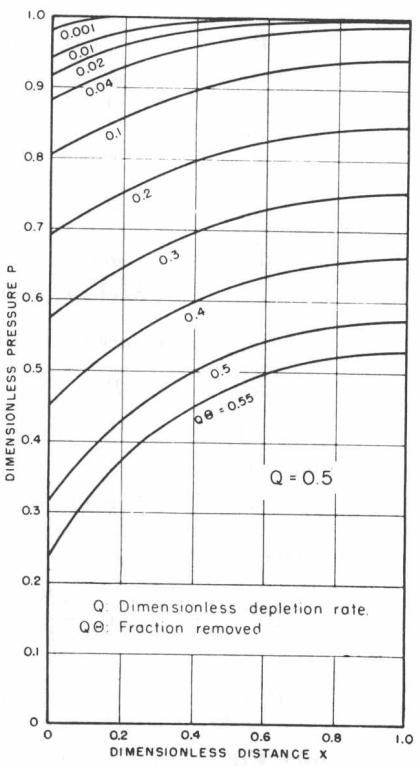

FIG. 3c — CALCULATED PRESSURE DISTRIBUTION FOR DEPLETION OF LINEAR GAS RESERVOIR. Q = 0.5.

was 20.58 ft. For the particular experiment considered, the porosity of the sand was 36.7 per cent; the permeability as determined by steady-state experiments was 13.2 md, with a variation of about 10 per cent from one end to the other. Nitrogen, originally at 108.1 psia, was produced from the sand at a constant rate of 0.000101 lb-mols per hour. The temperature was 78°F. For these conditions, $Q = 1.721$, and $\Theta = 0.0011525\,\theta$, where θ is expressed in minutes. The pressure distributions were calculated with the predictive equation, using 20 distance increments and $\Delta\Theta = 0.0005$. These are shown as smooth curves in Fig. 4. Comparison of these curves with the experimentally determined points shows the difference to be well within the experimental error.

RADIAL FLOW

The second case considered in this paper is that of radial flow with constant production rate. Equation (2′) reduces to

$$\frac{\partial^2 p^2}{\partial r^2} + \frac{1}{r}\frac{\partial p^2}{\partial r} = \frac{2\phi\mu}{K}\frac{\partial p}{\partial \theta} \quad . \quad . \quad . \quad . \quad . \quad (41)$$

with initial condition of Equation (7) and boundary conditions

$$r = r_q, \qquad q = \frac{K(2\pi r_q t)}{\mu RT}\, p\frac{\partial p}{\partial r} \quad . \quad . \quad . \quad (42)$$

$$r = r_b, \qquad p\frac{\partial p}{\partial r} = 0 \quad . \quad . \quad . \quad . \quad . \quad . \quad . \quad (43)$$

where r_q is the radius at which constant production rate is maintained, and r_b is the outer radius of the closed reservoir. By making substitutions

$$P = \frac{p}{p_i} \quad . \quad . \quad . \quad . \quad . \quad . \quad . \quad . \quad . \quad . \quad . \quad (10)$$

$$U = \log\,(r/r_b) \quad . \quad . \quad . \quad . \quad . \quad . \quad . \quad . \quad . \quad (44)$$

$$\Theta = \frac{p_i K\theta}{2r_b^2\phi\mu} \quad . \quad . \quad . \quad . \quad . \quad . \quad . \quad . \quad . \quad (45)$$

$$Q' = \frac{\dfrac{dN}{d\Theta}}{N_i} = \frac{2q\mu RT}{\pi p_i^2 Kt(1 - r_q^2/r_b^2)} = \frac{Q}{1 - r_q^2/r_b^2} \quad . \quad (46)$$

Equations (41) - (43) reduce to the dimensionless form

$$\frac{\partial^2 P^2}{\partial U^2} = e^{2U}\frac{\partial P}{\partial \Theta} \quad . \quad . \quad . \quad . \quad . \quad . \quad . \quad . \quad . \quad (47)$$

with initial condition

$$\Theta = 0, \qquad P = 1 \quad . \quad . \quad . \quad . \quad . \quad . \quad . \quad . \quad (15)$$

and boundary conditions

$$U = U_q = \log\,(r_q/r_b), \qquad \frac{\partial P^2}{\partial U} = \frac{Q}{2} \quad . \quad . \quad . \quad . \quad (48)$$

$$U = 0, \qquad \frac{\partial P^2}{\partial U} = 0 \quad . \quad . \quad . \quad . \quad . \quad . \quad . \quad . \quad . \quad (49)$$

Difference Equation

To approximate Equation (47) by a difference equation, a net of ΔU and $\Delta\Theta$ is chosen as before, with subscripts j and k used to denote mesh points in the U and Θ directions, respectively. Approximations to derivatives at j,k are found by the Taylor expansions of P^2 about j,k, as in Equations (18) and (19), with U substituted as the distance variable. If these modified equations are added, the result is

$$\Delta^2_{j,k} P^2 = 2\left(\frac{\partial^2 P^2}{\partial U^2}\,\frac{\overline{\Delta U}^2}{2!} + \frac{\partial^4 P^2}{\partial U^4}\,\frac{\overline{\Delta U}^4}{4!} + \ldots\right) \quad . \quad (50)$$

The ΔU of interest for a reasonable number of increments is larger than the corresponding ΔX of the linear case, and the U-derivatives are generally higher than the corresponding derivatives in X. For this reason, the approximations used for Equation (20) must be made higher-order correct. The higher-order terms in Equation (50) may be evaluated by differentiating Equation (47) with respect to U. The Z-th derivative may be expressed as

$$\frac{\partial^Z P^2}{\partial U^Z} = 2^{Z-2} e^{2U}\frac{\partial P}{\partial \Theta} + 2^{Z-3}(Z-2)\, e^{2U}\frac{\partial^2 P}{\partial U \partial \Theta} + \frac{2^{Z-4}(Z-2)(Z-3)}{2!} e^{2U}\frac{\partial^3 P}{\partial U^2 \partial \Theta} + \ldots \quad (51)$$

By letting

$$\psi = 2\sum_{Z=2,4\ldots}\frac{2^{Z-2}}{Z!}\overline{\Delta U}^Z \quad . \quad . \quad . \quad . \quad . \quad . \quad . \quad . \quad . \quad . \quad (52)$$

$$\lambda_j = \frac{2e^{2Uj}}{\Delta U \Delta\Theta}\sum_{Z=2,4\ldots}\frac{2^{Z-3}(Z-2)}{Z!}\overline{\Delta U}^Z \quad . \quad . \quad . \quad (53)$$

and

$$\sigma_j = \frac{e^{2Uj}}{\overline{\Delta U}^2 \Delta\Theta}\sum_{Z=2,4\ldots}\frac{2^{Z-4}(Z-2)(Z-3)}{Z!}\overline{\Delta U}^Z \quad . \quad (54)$$

and neglecting the terms $\dfrac{\partial^4 P}{\partial U^3 \partial \Theta}$ and higher in Equation (51), combination of Equation (50) and Equation (51) yields the difference approximation at j,k,

$$\Delta^2_{j,k}(P^2) - \lambda_j \Delta U \Delta\Theta \frac{\partial^2 P}{\partial U \partial \Theta} - \sigma_j \overline{\Delta U}^2 \Delta\Theta \frac{\partial^3 P}{\partial U^2 \partial \Theta} = \psi\frac{\partial^2 P^2}{\partial U^2} \quad . \quad (55)$$

Equation (55) may be combined with Equation (21) and Equation (47) to give a predictive difference equation. In this form, however, approximation of the crossed partial derivatives of Equation (55) is impossible. Moreover, the predictive form here has even more unfavorable mesh-ratio conditions than in the linear case, Equation (22), and is of little practical value. As shown in the Appendix, the condition sufficient to prevent error growth in the radial predictive case is approximately

$$\frac{\overline{\Delta U}^2}{\Delta\Theta} e^{2U_1} \geqslant 4P_k \quad . \quad . \quad . \quad . \quad . \quad . \quad . \quad . \quad . \quad . \quad (56)$$

For a practical case, r_q/r_b may be 1/200, so that U_1 is 0.975 log (1/200) or −5.17 in a 20-increment net, and $\Delta U = -(1/20)$ log (1/200) or 0.265. The value of $\overline{\Delta U}^2 e^{2U_1}$ is 2.26×10^{-6} or $\Delta\Theta < 5.65 \times 10^{-7}$ when P is 1.0. With such a small $\Delta\Theta$, at $Q = 0.01$, over 88 million time steps would be required to remove half the gas.